Quaternary and Neogene Reservoirs of the Norwegian Continental Shelf and the Faroe-Shetland Basin

Bellwald, B.[1,2,3], Planke, S.[1,2,3], Vadakkepuliyambatta, S.[4,5], Buenz, S.[4], Batchelor, C.[6], Manton, B.[1], Zastrozhnov, D.[1,7,8], Walker, F.[1], Garcia, A.[3], Myklebust R.[9], Kjølhamar, B.[9]

Abstract

Glaciogenic reservoirs host important hydrocarbon resources across the globe. Examples such as the Peon and Aviat discoveries in the North Sea show that Quaternary and Neogene reservoirs can be prospective in the region. In this study, we interpret 2D and 3D reflection seismic data combined with borehole information to document unconventional play models from the shallow subsurface of the Norwegian Continental Shelf and the Faroe-Shetland Basin. These plays include (i) glacial sands in ice-marginal outwash fans, sealed by stiff subglacial tills (the Peon discovery), (ii) meltwater turbidites, (iii) contouritic fine-grained glacimarine sands sealed by gas hydrates, (iv) remobilized oozes above large evacuation craters which are sealed by megaslides and glacial muds, and (v) Neogene sand injectites. The hydrocarbon reservoirs are characterized by negative-polarity reflections with anomalously high amplitudes in the reflection seismic data as well as density and velocity decreases in the borehole data. Extensive new 3D reflection seismic data are crucial to correctly interpret glacial processes and distinguish shallow reservoirs from shallow seals. These data document a variety of play models with the potential for gas in large quantities and enable the identification of optimal drilling targets at stratigraphic levels which have so far been overlooked.

[1]Volcanic Basin Energy Research (VBER), Oslo, Norway

[2]Fjorgyn, Oslo, Norway

[3]University of Oslo, Norway

[4]Centre for Arctic Gas Hydrate, Environment and Climate (CAGE), Department of Geosciences, UiT-The Arctic University of Norway, Tromsø, Norway

[5]National Centre for Polar and Ocean Research, Ministry of Earth Sciences, Vasco-da-Gama, Goa, India

[6]Newcastle University, Newcastle upon Tyne, UK

[7]Institute of Earth Sciences, Saint Petersburg State University, Saint Petersburg, Russia

[8]A.P. Karpinsky Russian Geological Research Institute, Saint Petersburg, Russia

[9]TGS, Asker, Norway

1. Introduction and study area

Neogene reservoirs account for 22.3 % of deep oil and gas in the world, and the undiscovered Neogene hydrocarbon reservoirs across the globe are estimated to ~5 billion barrels of oil equivalent (Ahlbrandt et al., 2005; Bai and Cao, 2014). Hydrocarbon accumulations in glaciogenic reservoirs are known from Paleozoic sandstones in South America, Australia, North Africa and the Middle East (Bache et al., 2012; Douillet et al., 2012; Girard et al., 2012; Huuse et al., 2012), and the potential of Quaternary glacial reservoirs has been highlighted in recent studies (Kurjanski et al., 2020). Shallow gas in glacial deposits can act as an energy resource for offshore industries, but can also constitute a potential drilling hazard for marine activities (Huuse et al., 2012).

The Norwegian Continental Shelf and Faroe-Shetland Basin are prospective petroleum provinces (Fig. 1), where most discoveries have been made in the Paleocene to Jurassic stratigraphic intervals (www.npd.no). Despite an overburden thickness of 200 to 2000 m, which is dominated by glacial muds, unconventional shallow reservoirs have been underestimated in prospectivity evaluations. Discoveries within the shallow subsurface include the Peon and Aviat fields within the Quaternary, the Liatårnet discovery in the Early Miocene, as well as the Alvheim field in the Neogene (www.npd.no). Shallow-gas closures are of structural, stratigraphic or lithological origin.

The Quaternary stratigraphy along the previously glaciated NE Atlantic margins comprises several hundred meters thick packages of glacigenic sediments, all belonging to the Naust Formation along the mid-Norwegian margin (Rise et al., 2005; Ottesen et al., 2009). Although these sediments are dominated by densely packed glacial muds, they vary strongly in grain size from fine-grained clay to coarse-grained sand (Batchelor et al., 2021). The underlying pre-glacial stratigraphic intervals are dominated by biosiliciclastic oozes, shales and sandstones of the Neogene Kai and Paleogene Brygge formations (Riis et al., 2005; Eidvin et al., 2007; Millett et al., 2020). Rapid glacial sedimentation had implications for fluid migration and overpressure build-up both within the Brygge Formation and the Naust Formation (Riis et al., 2005; Lawrence and Cartwright, 2010; Bellwald et al., 2019).

Submarine fans of fluvial origin are proven exploration targets (e.g., Nile, Mississippi, and Niger fans), whereas the potential of their glacial counterparts, called trough mouth fans, has so far been overlooked. Large 3D reflection seismic cubes from the underexplored slope domains of the NE Atlantic margin are available since 2017 (Fig. 1), and allow imaging Quaternary processes in high resolution (Bellwald et al., 2020). Seismic data is the primary tool for identifying shallow gas over larger areas or in smaller accumulations, and common evaluation criteria are negative-polarity reflections with anomalously high amplitudes (Heggland, 2004). Here, we present new Quaternary and Neogene play models from the Norwegian Continental Shelf and Faroe-Shetland Basin based on the interpretation of new high-quality 3D reflection seismic data, high-resolution 3D P-Cable reflection seismic data, seismic velocity data, as well as geological and geophysical well ties (Fig. 1; Tab. 1).

2. Data and methods

We use high-resolution 3D P-Cable reflection seismic data (Figs. 2, 3), industry-processed high-quality 3D reflection seismic data (Fig. 4), and well logs to characterize the Neogene and Quaternary reservoirs and seals along the NE Atlantic margins (Fig. 1; Tab. 1). The dataset includes three large seismic volumes covering an area of c. 80,000 km^2 on the continental slopes of the North Sea Fan area as well as the Faroe-Shetland Basin.

A high-resolution volume at 2 ms sample rate and 6.25 x 18.75 m bin size was designed to increase the resolution of the shallow stratigraphy of the conventional datasets. The data for the high-resolution volume have been cut at either of twice the seabed time or 5000 ms two-way time before zero-phasing. This high-resolution volume has a vertical resolution of c. 2 m (Fig. 4). While no spatial or temporal resampling has been applied on the high-resolution volume, limited noise removal and de-multiple have been applied. The intermediate fast-track version of the data, in comparison, have been resampled at 37.5 m x 37.5 m and a temporal sampling that gave a vertical resolution of c. 8 m within the Late Cenozoic stratigraphy. In addition, a high-resolution 3D P-Cable reflection seismic cube with an extent of 150 km^2, a horizontal resolution of 6 m and a vertical resolution of 2 m has been interpreted to highlight shallow prospectivity in the northern North Sea (Figs. 2, 3). The AM datasets have all American polarity, whereas EWW18 and the P-Cable datasets have European polarity (Fig. 1). In the illustrations in this paper reflections caused by an increase in acoustic impedance, positive-amplitude reflections, are shown as black in profiles while the opposite, reflections caused by a decrease in acoustic impedance, negative-amplitude reflections, are shown as white.

Depth processing to optimally image the complex geology of the Faroe-Shetland Basin was achieved with a combination of careful pre-processing and velocity-model building, incorporating an efficient high-resolution velocity model building method, guided tomography, and Dynamic Matching Full Waveform Inversion (DM FWI). For DM FWI, both reflection and refraction information are used. A tilted transverse isotropy Kirchhoff post-stack depth migration route was chosen, with the focus on a very detailed pre-processing sequence and advanced velocity model building.

Detailed horizon picking (line spacing of 50 m), gridding and attribute analysis as well as seismic geomorphological interpretation have been conducted to characterize hydrocarbon plays in the shallow subsurface (Tab. 1). We defined seismic and sedimentary facies, identified facies boundaries and architectural elements, and established a depositional history and formation model for the fans. The interpreted horizons were tied to the Peon (35/2-1), Havsule (6404/11-1), Solsikke (6403/10-U1), Tobermory (214/4-1), and Bunnehaven (214/9-1) wells, for which geophysical and biostratigraphical information are available using the Facies Map Browser (FMB) of TGS.

3. The Peon gas discovery: A glacial outwash fan sealed by stacked sequences of glacial till

The Peon gas discovery in the northern North Sea consists of an up to 50 m thick sandstone sequence (Fig. 2) with c. 20 x 10^9 standard m^3 of recoverable gas (www.npd.no). Borehole 35/2-1 penetrates the Peon sandstone for c. 30 m at a location where the reservoir sandstone is not at its thickest. High-resolution 3D P-Cable reflection seismic data show that the Peon discovery is characterized by a high-amplitude, negative-polarity reflection at the top of the reservoir and a seismic no-reflection zone within the sandstone reservoir (Fig. 2a). The sandstone, which is deposited directly above a glacial unconformity (Upper Regional Unconformity, URU) at a subsurface depth of c. 200 m, is overlain by eight units of subglacial till and glacimarine sediment, separated by high-amplitude seismic reflections of both polarities (Fig. 2a, H1-H7). Iceberg ploughmarks (identified at H1, H3, H5-7; Figs. 2c, 3), glacial lineations (H1-2; Figs. 2c, 3b), and pockmarks (H1-H3, H5-H7; Figs. 2c, 2d, 3b) are expressed on the grids of these seven horizons within the overburden. Borehole 35/2-1 shows that the overburden is dominated by muddy sediments with densities >2.2 g/cm^3, sonic velocities >1.6 km/s, and gamma-ray values of c. 90 GAPI (Fig. 2b). For the glacigenic sediments directly above the top reservoir, sonic velocities >2.1 km/s and densities of up to 2.4 g/cm^3 are measured. In contrast, the reservoir is characterized by sandy sediments with densities of c. 2 g/cm^3, sonic velocities <1 km/s, and gamma-ray values of c. 60 GAPI (Fig. 2b). The gas-water contact is located c. 5 m above the glacial unconformity, and correlates with a high-amplitude reflection of positive polarity at the well location. Although dominated by glacial muds, more coarse-grained beds are drilled at certain intervals of the overburden (e.g., H7). In between H4 and H5, we observe chaotic shallow seismic anomalies, c. 40 m above the top of the reservoir (Figs. 2a, 3c).

We interpret that the Peon reservoir is a gas-charged porous sandy outwash fan formed in the Norwegian Channel at the ice-stream margin of the Fennoscandian Ice Sheet (Fig. 3a). Proglacial outwash plains with channelized sandstone bodies build the Late Ordovician hydrocarbon reservoirs in the Tassili N'Ajjer, Algeria and Libya, North Africa (Girard et al., 2012). The reservoir consists of unconsolidated glacial sands, as indicated by very low sonic velocities and densities (Fig. 2b), and is typically seen as a no-reflection zone in the seismic profiles. The overburden of the Peon reservoir consists of stacked units of overconsolidated subglacial till and glacimarine sediment, formed during ice-sheet oscillations (Sejrup et al., 1994), which slightly modified the shape of the reservoir (Fig. 3b). The charging of the Pleistocene reservoir occurred through vertical fluid flow and along pre-Quaternary progrades below the glacial unconformity, which are visible as dipping reflections of moderate to high amplitudes (Fig. 2a). The presence of hydrocarbons and a hydrocarbon-charged Peon reservoir are shown by the shallow seismic anomalies above the Peon outwash fan (Figs. 2a, 3c). In addition, pockmarks at different subsurface levels and at the seabed indicate fluid leakage from the gas-charged Peon field (Figs. 2a, 2c, 2d, 3b). Fluids thus migrated into the shallow subsurface as well as into the water column. Shallow anomalies and pockmark fields above hydrocarbon reservoirs have been observed in different areas of

the Norwegian Continental Shelf, including at the Troll and Snøhvit fields (Mazzini et al., 2016; Tasianas et al., 2018).

4. Meltwater turbidites

The uppermost unit of the North Sea Fan is characterized by an up to 400 m thick sediment package, reaching from the top of the Tampen Slide to the seabed (Fig. 4). This unit is discussed in detail in a previous study (Bellwald et al., 2020), and we here summarize the relevance of this package for offshore prospectivity. High-resolution processed 3D seismic data reveal that seven continuous, high-amplitude reflections interrupt the otherwise homogenous sediment package (Fig. 4). These reflections are of both negative and positive polarities, and separate the package into eight sub-units with thicknesses of 20 to 80 m. Deep, 'v'-shaped depressions are commonly observed along the high-amplitude reflections, locally truncating underlying reflections. These high-amplitude reflections are interpreted as surfaces of channel-levee systems along a gently-dipping seabed (Fig. 5). The channels have an elongated geometry and originate from multiple source areas on the paleo-shelf (Fig. 5a) (Bellwald et al., 2020). Following these channels downslope, the channels diverge and converge within short distances for total lengths of >150 km. The channels are 4 to 100 m deep and 90 to 2100 m wide.

The channels are characterized by high-amplitude reflections compared to the well-developed low-amplitude elongated levees between the channels (Fig. 5b). Seven horizons showing such channel-levee systems can be seen in Fig. 4b. The strong positive and negative impedance contrasts characterizing these seismic horizons originate from changes in density and/or velocity, and indicate coarser-grained sediment in active channels overlying more fine-grained sediments (Bellwald et al., 2020). These more fine-grained deposits with transparent seismic facies could also represent glacigenic debris flows (Nygård et al., 2005). Studies from the Labrador Sea show that glacial turbidites can consist of medium-grained sand and coarser sediments (Hesse et al., 1997). The levees, in contrast, indicate fine-grained sediment deposits originating from the suspensive load associated with hyperpycnal flows. Channels infilled by loose sands may show negative polarities with respect to the host beds (Figs. 4b, 5). The overflowing levees that formed by the suspensive load show lower impedance contrasts, and most likely consist of sediments similar to the glacial muds of the host beds.

The stacked channel-levee systems are a result of several sedimentation pulses characterized by rapid coarse-grained sediment input from the Norwegian Channel Ice Stream (Bellwald et al., 2020). The channels document long-distance sediment transport in completely disintegrated water-rich turbidite flows. These turbidite currents were most likely high-density and sand-rich mass movements, similar to the deposits reported by Hesse et al. (1997) from the Labrador Sea. Stratigraphic units comparable to the uppermost sediment sequence dominated by stacked channel-levee systems are further identified at deeper levels of the North Sea Fan.

Deep-water processes in submarine fans of glacial origin allow long-distance sediment transport and sediment sorting. Sands deposited by meltwater turbidites in channel-levee systems on the upper slopes

of the North Sea Fan are potential hydrocarbon reservoirs. These reservoirs are sealed by fine-grained glacial sediment of low permeability and low porosity, including glacial muds, glacigenic debris, and slides. Glacial meltwater was crucial for the formation of the Late Paleozoic glaciogenic valleys and fills that act as hydrocarbon reservoirs in the Chaco Basin, onshore Bolivia (Bache et al., 2012).

5. Contouritic sands sealed by gas hydrates and fine-grained debris flows

Gas hydrates and associated free gas are thought to impact global climate, affect slope stability, and furthermore act as a potential energy resource (Kvenvolden, 1993). Geophysical evidence for gas hydrates is widespread along the northern flank of the Storegga Slide, where a bottom simulating reflection (BSR) at the base of the gas-hydrate stability zone covers an area of approximately 4000 km^2 (Buenz et al., 2003). A negative-polarity BSR cross-cutting the strata in the eastern part of the AMN17 3D survey c. 280 to 420 ms below seafloor is reported where high-amplitude reflections occur below low-amplitude reflections (Buenz et al., 2003). Similar to the results of Buenz et al. (2003), the BSR in our study is mainly shown as an envelope of increased reflection terminations (Fig. 6a). The BSR is only in few places exhibited as a reflection proper of reversed phase when compared to the seafloor reflection. A BSR crosscutting through different layers of the Quaternary stratigraphy in the Nyegga area has been documented by several studies before (e.g., Plaza-Faverola et al., 2010; Hjelstuen et al., 2010), whereas the BSR is less evident if the stratigraphy is bedded parallel to the seafloor.

The high-amplitude reflections below the BSR follow the eastwards-dipping stratigraphy and are truncated by the BSR to the west. We interpret these continuous strong, negative-amplitude reflections as gas-charged sandy sediments of contouritic origin. A contouritic origin of the sediment package is supported by its geometry, particularly the constant thickness and the continuous-amplitude reflections forming the package (Figs. 6, 7). The location of the site within the paleogeographic setting makes it further unlikely for the package to be dominated by downslope deposits, as there is no glacial fan located in the direct vicinity (Fig. 1). The BSR most likely represents the contact between gas hydrates and free gas, as suggested for the Nyegga area on the southern Vøring Margin, where average free-gas concentrations are approximately 0.4 to 0.8 % of the pore volume (Buenz et al., 2005). Geophysical investigations from the Nyegga area further show that the sediments below the BSR, characterized by high-amplitude reflections, have lower velocities compared to the sediments above the BSR (e.g., Buenz et al., 2005; Plaza-Faverola et al., 2010). Thus, gas-hydrated sediments act as a seal for stratigraphy-bound free gas below. The BSR seals gas within estimated 60 m thick beds over an extent of c. 1400 km^2 for the Naust U sub-unit, and the rock reservoir volume is estimated as 132 x 10^9 km^3 (Fig. 6b). Additional potential gas reservoirs are suggested in more porous glacimarine sediments at the base of Naust T, in the lower part of Naust S, at the base of Naust U, and at the top of Naust N/A (Figs. 6b; 7a).

Upward-bending reflections cutting continuously deposited glacimarine sediments are interpreted as blow-out pipes (Fig. 7a). These blow-out pipes end at the seafloor, where they are associated with depressions identified as pockmarks. The pipes indicate overpressured layers at shallow levels as well

as gas-hydrate seal breach at several locations, as proposed in previous studies of the mid-Norwegian margin (Buenz et al., 2003; Berndt, 2005), and may thus represent a potential geohazard. The pipe structures rise from >2.1 s twt, corresponding to 800 m bsf, to the seabed (Fig. 7a). These pipes correlate with the location of seabed pockmarks in water depths of 800 to 1000 m (Fig. 7b), and are another indicator of fluid-escape from overpressured layers. Free gas beneath the gas-hydrate stability zone and associated features (gas-escape pipes and pockmarks) could thus indicate seepage of thermogenic gas from depth.

Contourites have an economic relevance for the offshore industries by acting both as reservoir and seal rocks (Viana et al., 2007). Contourites of Plio-Pleistocene age have been identified in the Faroe-Shetland Channel and the northern North Sea area, with lithologies varying from muddy to sandy grain size (Knutz and Cartwright, 2003; Batchelor et al., 2017; 2021). In the Storegga Slide area, contouritic sediments are suggested to act as reservoir rocks for fluids sealed by the BSR. Sourced from the East Shetland Platform and the northern North Sea (Batchelor et al., 2021), the contour currents transported the available sediments northwards, where the regional physiography enhanced the ocean currents and hosted contouritic deposition. Furthermore, downslope-processes active on the North Sea Fan could have acted as an additional source for the sandy load of the contourites (Bellwald et al., 2020). The contourites of the Pliocene to Quaternary are characterized by continuously laminated sediments, and most likely contain gas-charged sands in selected locations.

6. Remobilized oozes

The Base Naust reflection from the North Sea Fan to the mid-Norwegian margin separates the biosiliciclastic oozes of the Paleogene-Neogene Brygge and Kai formations from the glacigenic sediments of the Quaternary Naust Formation and is characterized by large evacuation structures with depths of c. 200 m (Fig. 8) (Riis et al., 2005; Lawrence and Cartwright, 2010). The base of the evacuation structures correlates with the depth of the Opal A/CT boundary (Fig. 8). These evacuation structures correlate with chaotic mounds identified in several levels of the stratigraphy above. The reflection defining the top of the mounds is the strongest negative-amplitude reflection in the uppermost two kilometers of the stratigraphy. The mounds have very strong negative-amplitude reflections with lower DM FWI velocities than the surrounding glacigenic sediments (Figs. 8, 9). These mounds are up to 300 m thick, have extensions of 1 to 150 km^2 and represent the remobilized oozes of the craters. Wireline log data from the Havsule and Solsikke wells show a strong density decrease from the overlying glacigenic sediments into the remobilized oozes (from 2.1 g/cm^3 to 1.2-1.5 g/cm^3, Fig. 10) (Riis et al., 2005), and a strong decrease in DM FWI velocities (Fig. 9). The low acoustic impedances of the mounds could result from the preglacial origin of the biosiliciclastic oozes as well as the potential presence of gas trapped below the overlying glacial sediments. The internal character of the mounds is characterized by a positive-amplitude reflection, which indicates either a change in lithology or a fluid contact within the crater infill (Figs. 8, 10). A fluid contact would rather be expressed as a flat event in

the seismic data, and a change in lithology correlates with the positive-amplitude reflection in the ooze mounds penetrated in the Solsikke well (6403/10-U1, Fig. 10), and we therefore interpret this positive-amplitude reflection to more likely represent a change in lithology. Structural maps of the top of the evacuation structures allow the remobilized oozes with a rough morphology to be distinguished from the neighboring glacimarine sediments with a smooth morphology (Fig. 8). We suggest that these mounds were formed by abrupt events of overpressure release.

Subsequent gas migration most likely charged these remobilized oozes, and is expressed by a strong negative-amplitude reflection at their upper surfaces and low DM FWI velocities within these bodies. Rapidly-deposited, low-permeability, and low-porosity glacial sediments seal overpressure originated from the fluids expelled from the underlying, high-permeable and highly-compressible biosilicious oozes (Kvalstad et al., 2005). Fluid sources include domes, reutilized hydrothermal vent complexes, compressible oozes, and expulsion related to the Opal A/CT transition.

7. Sand injectites

Sand injectites form by fluidization of sand, often in response to the failure of a low-permeability sealing lithology (Hurst et al., 2005). Sand injectites are increasingly viewed as potential exploration targets with high-quality reservoirs formed by remobilization processes that separate sand from finer grained material (Jolly and Londergan, 2002; Hurst et al., 2005; Løseth et al., 2013; Skjærpe et al., 2018). They often intrude mudstones which form high-quality seals (Cartwright, 2010). How sand injectites connect to depositional sand units and how they interconnect with each other is significant in terms of reservoir volumes and for potential fluid contacts (Cartwright et al., 2007).

7.1 Southern Møre Basin

At the uppermost slopes of the North Sea Fan into the northern North Sea an area of c. 3,600 km^2 at a subsurface depth of c. 2 km is characterized by structures with a chaotic internal seismic facies (Fig. 11). The geometry of these chaotic expressions varies from saucer-shaped reflections to laterally extensive reflections to clusters of reflections (Figs. 11, 12). These structures crosscut more than 300 m of continuous high-amplitude reflections of the Eocene-Oligocene Brygge Formation (Figs. 12b, 13), cutting the Top Oligocene reflection and almost reaching the Base Naust reflection (Figs. 11, 12). The chaotic seismic facies occurs above the level of the diagenetic Opal A/CT reflection, although this reflection is often disrupted where injectites are present. The acoustically chaotic bodies are surrounded by upward-bending beds and have occasionally strong negative-amplitude top reflections, directly underlain by strong positive-amplitude reflections. (Figs. 11, 12).

The reflections in the chaotic seismic facies have typical geomorphologies for sand injectites (e.g., Bureau et al., 2013). We therefore suggest that these chaotic facies are formed by the injection of fluidized sand. We interpret these sand injectites to have an estimated reservoir thickness of c. 50 m, which is similar to extensively mapped sand injectites in the upper Pliocene of the North Sea

(Cartwright, 2010). Additionally, the chaotic seismic facies contains clusters of incoherent reflections, which are several hundred meter thick, with similar amplitudes, and a close association to the saucer-shaped reflections (Fig. 11). These characteristics suggest they are also injectites that are not fully resolved in the seismic data. The clusters could represent interconnected injectite swarms such as those observed in the Panoche Hills, California (Vétel and Cartwright, 2010), and may be veins at a sub-seismic scale.

The sand injectites are trapped structurally by the surrounding Paleogene oozes. The injectites are most likely sourced from Eocene sands (Top Balder), mid-Campanian sands (Top Nise), or remobilized local Oligocene sands (Fig. 11). The injectites are probably characterized by good connectivity and permeability (Figs. 11, 12). Paleogene beds also act as mother beds for the high-permeability and high-connectivity injected sands forming the Volund and Viper-Kobra fields in the Alvheim area (Skjærpe et al., 2018).

The base of the sand injectite bodies correlates with the base of the ooze-evacuation structures. We therefore suggest that the evacuation structures and injectites are associated, and that both injectite movement and ooze remobilization occurred in response to Quaternary sedimentation. Remobilization processes, related to rapid glacial sedimentation and associated overpressure build-up, have been modelled for the megaslides of this region (Bellwald et al., 2019).

7.2 Faroe-Shetland Basin

Similarly to the Møre Basin, sand injectites are interpreted in the northern Faroe-Shetland Basin (EWW18 3D survey) based on their high-amplitude negative-amplitude reflections, which are caused by their low acoustic impedances (Fig. 14a, 14b) (Hurst et al., 2005). They commonly have ‘v’-shaped geometries and more rarely ‘saucer-shaped’ geometries with flat bases and rising wings (Fig. 14b). These sand injectites are geometrically somewhat similar to igneous sills, as they are concave-upwards and saucer-shaped expressions ending abruptly, and are characterized by high-amplitude seismic reflections. Compared to the igneous sills, the sand injectites occur shallower in the geological succession and are about a tenth of their diameter (generally less than 5 km across), which is consistent with global observations (Polteau et al., 2008). Unlike in the Møre Basin the sand injectites in EWW18 nearly entirely occur below the Opal A/CT reflection.

In the central part of EWW18, there is a seismically distinct unit that consists of high-amplitude, relatively coherent reflections, which occur in lenticular bodies. These bodies are interpreted to be lobes of the sand-rich mid-Eocene Strachan Fan (Figs. 14a, 15) (Stoker et al., 2018). The fan consists of several lobes, which reach thicknesses of up to 340 ms in EWW18 (Figs. 14a, 15). The Tobermory gas discovery (214/4-1) occurs within sandstone intervals of the northern lobe of the Strachan Fan (Fig. 14a) (cf. Schofield et al., 2017).

The sand injectites in EWW18 can be characterized based on their stratigraphic level: shallow injectites in the stratigraphy above the Strachan Fan, and deep injectites in the stratigraphy below the fan (Fig. 14a). Stratigraphically deeper sand injectites are penetrated at both the Tobermory (214/4-1) and Bunnehaven wells (214/9-1) (Fig. 14c, d). The stratigraphically shallower sand injectites above the Strachan Fan have stronger amplitude responses than the stratigraphically-deeper sand injectites below the fan, and are generally distinct singular reflections (Fig. 14a, b). Many of the sand injectites occur directly above the southern lobe of the Strachan Fan suggesting the fan lobe is the source of the sand. The top of the southern lobe of the Strachan Fan has a high negative-amplitude response (Fig. 15b) suggesting it is gas charged akin to the northern lobe. However, some of the charge may have migrated into the connected injectites.

7.3 Sand injectites synthesis

The sand injectites in both study areas occur above the Balder Formation (early Eocene) and below Base Pleistocene (Base Naust Formation in the Norwegian sector). In both study areas there is a very positive-amplitude reflection that crosscuts the stratigraphy (Figs. 10, 11, 14), including the Opal A/CT diagenetic boundary (Brekke, 2000; Berndt et al., 2004; Lawrence and Cartwright, 2009). The interconnectedness of the injectites is significant from a reservoir evaluation perspective for both areas. In the Faroe-Shetland Basin, the injectites connect to the top of the Strachan Fan (Fig. 14a, b), increasing its reservoir volume and suggesting hydrocarbons may occur above the structural high of the fan. In the North Sea Fan, the injectites appear to be highly connected (Figs. 12, 13), suggesting hydrocarbons may be able to migrate significant distances through the injectite clusters.

The differences in geometries of the injectites in the two study areas may be related to their relationships to the Opal A/CT transition (Figs. 11, 14a). The close relationship between the locations of the injectites and the Opal A/CT transition suggests that the Opal A/CT transition was located at its current position at the time of the shallowest sand injection. The Opal A/CT transition has been fossilized since the Neogene along much of the Atlantic margin (Neagu et al., 2010). The mineralization process at the Opal A/CT transition may form more brittle rocks below the boundary, leading to more distinct sheet-shaped intrusions. In contrast, the mudstones above the Opal A/CT transition may be less structurally coherent when the injectites were emplaced leading to more complex geometries.

8. Conclusions

The development of the Fennoscandian and British ice sheets resulted in a rich variety of depositional environments with lateral and spatial changes in sedimentary deposits. The rapidly-deposited and several kilometers thick Quaternary sequence had significant implications on overpressure development in the underlying Cenozoic sequences. The Quaternary and Neogene stratigraphy of the Norwegian Continental Shelf and the Faroe-Shetland Basin comprises several unconventional hydrocarbon plays characterized by prominent anomalies in both seismic and borehole data (Tab. 1). The region has a significant potential for unconventional sandstone reservoirs in the Quaternary and Neogene, with plays

spanning large areal extents and significant volumes. Different play types are identified at the same geographic locations, but at different stratigraphic intervals. These plays could therefore be tested by single wells targeting multiple stratigraphic levels. Seismic attribute analysis and geomorphological interpretation display major lateral variations along the mapped horizons. The use of new and extensive high-quality 3D seismic data is crucial to correctly interpret geological processes forming such shallow reservoirs and to identify fluid accumulations, estimate reservoir volumes, and select optimal drilling locations. These Quaternary and Neogene reservoirs are not only relevant for hydrocarbon exploration, but are also potential targets for carbon storage as well as sources of greenhouse gases.

Acknowledgements

We thank TGS and Equinor for allowing us to publish the seismic profiles and seismic images.

References:

Ahlbrandt, T. S., Charpentier, R. R., Klett, T. R., Schmoker, J. W., Schenk, C. J. and Ulmishek, G. F. [2005] Global Resource Estimates from Total Petroleum Systems. *AAPG Memoir*, **86**, AAPG.

Bache, F., Moreau, J., Rubino, J. L., Gorini, C. and Lanoë, B. V. V. [2012] The subsurface record of the Late Palaeozoic glaciation in the Chaco Basin, Bolivia. *Geological Society, London, Special Publications*, **368(1)**, 257-274.

Bai, G. P. and Cao, B. [2014] Characteristics and distribution patterns of deep petroleum accumulations in the world. *Oil Gas Geol*, **35(1)**, 19-25.

Batchelor, C. L., Bellwald, B., Planke, S., Ottesen, D., Henriksen, S., Myklebust, R., ... and Dowdeswell, J. A. [2021] Glacial, fluvial and contour-current-derived sedimentation along the northern North Sea margin through the Quaternary. *Earth and Planetary Science Letters*, **566**, 116966.

Batchelor, C. L., Ottesen, D. and Dowdeswell, J. A. [2017] Quaternary evolution of the northern North Sea margin through glacigenic debris-flow and contourite deposition. *Journal of Quaternary Science*, **32(3)**, 416-426.

Bellwald, B., Planke, S., Becker, L. W. and Myklebust, R. [2020] Meltwater sediment transport as the dominating process in mid-latitude trough mouth fan formation. *Nature communications*, **11(1)**, 1-10.

Bellwald, B., Urlaub, M., Hjelstuen, B. O., Sejrup, H. P., Sørensen, M. B., Forsberg, C. F. and Vanneste, M. [2019] NE Atlantic continental slope stability from a numerical modeling perspective. *Quaternary Science Reviews*, **203**, 248-265.

Berndt, C. [2005] Focused fluid flow in passive continental margins. *Philosophical Transactions of the Royal Society A: Mathematical, Physical and Engineering Sciences*, **363(1837)**, 2855-2871.

Berndt, C., Bünz, S., Clayton, T., Mienert, J. and Saunders, M. [2004] Seismic character of bottom simulating reflectors: examples from the mid-Norwegian margin. *Marine and Petroleum Geology*, **21(6)**, 723-733.

Brekke, H. [2000] The tectonic evolution of the Norwegian Sea continental margin, with emphasis on the Voring and More basins. *Special Publication-Geological Society of London*, **167**, 327-378.

Buenz, S., Mienert, J., Vanneste, M. And Andreassen, K. [2005] Gas hydrates at the Storegga Slide: Constraints from an analysis of multicomponent, wide-angle seismic data. Geophysics, **70(5)**, B19-B34.

Buenz, S., Mienert, J. and Berndt, C. [2003] Geological controls on the Storegga gas-hydrate system of the mid-Norwegian continental margin. *Earth and Planetary Science Letters*, **209(3-4)**, 291-307.

Bureau, D., Mourgues, R., Cartwright, J., Foschi, M., and Abdelmalak, M. M. [2013] Characterisation of interactions between a pre-existing polygonal fault system and sandstone intrusions and the

411 determination of paleo-stresses in the Faroe-Shetland basin. *Journal of Structural Geology*, **46**,
412 186-199.
413 Cartwright, J. [2010] Regionally extensive emplacement of sandstone intrusions: a brief review. *Basin*
414 *Research*, **22(4)**, 502-516.
415 Cartwright, J., Huuse, M. and Aplin, A. [2007] Seal bypass systems. *AAPG Bulletin*, **91(8)**, 1141-1166.
416 Douillet, G., Ghienne, J. F., Géraud, Y., Abueladas, A., Diraison, M. and Al-Zoubi, A. [2012] Late
417 Ordovician tunnel valleys in southern Jordan. *Geological Society, London, Special Publications*,
418 **368(1)**, 275-292.
419 Eidvin, T., Bugge, T. and Smelror, M. [2007] The Molo Formation, deposited by coastal progradation
420 on the inner Mid-Norwegian continental shelf, coeval with the Kai Formation to the west and the
421 Utsira Formation in the North Sea. *Norwegian Journal of Geology/Norsk Geologisk Forening*,
422 **87**.
423 Girard, F., Ghienne, J. F. and Rubino, J. L. [2012] Channelized sandstone bodies ('cordons') in the
424 Tassili N'Ajjer (Algeria & Libya): snapshots of a Late Ordovician proglacial outwash plain.
425 *Geological Society, London, Special Publications*, **368(1)**, 355-379.
426 Heggland, R. [2004] Definition of geohazards in exploration 3-D seismic data using attributes and
427 neural-network analysis. *AAPG bulletin*, **88(6)**, 857-868.
428 Hesse, R., Khodabakhsh, S., Klaucke, I. and Ryan, W. B. [1997] Asymmetrical turbid surface-plume
429 deposition near ice-outlets of the Pleistocene Laurentide ice sheet in the Labrador Sea. Geo-
430 Marine Letters, **17(3)**, 179-187.
431 Hjelstuen, B. O., Haflidason, H., Sejrup, H. P. and Nygård, A. [2010] Sedimentary and structural control
432 on pockmark development—evidence from the Nyegga pockmark field, NW European margin.
433 *Geo-Marine Letters*, **30(3)**, 221-230.
434 Hurst, A., Cartwright, J. A., Duranti, D., Huuse, M. and Nelson, M. [2005] Sand injectites: an emerging
435 global play in deep-water clastic environments. In *Geological Society, London, Petroleum*
436 *Geology Conference series*, **6(1)**, 133-144.
437 Huuse, M., Le Heron, D. P., Dixon, R., Redfern, J., Moscariello, A. and Craig, J. [2012] Glaciogenic
438 reservoirs and hydrocarbon systems: an introduction. *Geological Society, London, Special*
439 *Publications*, **368(1)**, 1-28.
440 Jolly, R. J. and Lonergan, L. [2002] Mechanisms and controls on the formation of sand
441 intrusions. *Journal of the Geological Society*, **159(5)**, 605-617.
442 Knutz, P. C. and Cartwright, J. [2003] Seismic stratigraphy of the West Shetland Drift: Implications for
443 late Neogene paleocirculation in the Faeroe-Shetland gateway. *Paleoceanography*, **18(4)**.
444 Kurjanski, B., Rea, B. R., Spagnolo, M., Cornwell, D. G., Howell, J. and Archer, S. [2020] A conceptual
445 model for glaciogenic reservoirs: from landsystems to reservoir architecture. *Marine and*
446 *Petroleum Geology*, **115**, 104205.

Kvalstad, T. J., Andresen, L., Forsberg, C. F., Berg, K., Bryn, P. and Wangen, M. [2005] The Storegga slide: evaluation of triggering sources and slide mechanics. *Marine and Petroleum Geology*, **22**, 245-256.

Kvenvolden, K. A. [1993] Gas hydrates—geological perspective and global change. *Reviews of geophysics*, **31(2)**, 173-187.

Lawrence, G.W.M. and Cartwright, J.A., [2010] The stratigraphic and geographic distribution of giant craters and remobilised sediment mounds on the mid Norway margin, and their relation to long term fluid flow. *Marine and Petroleum Geology*, **27(4)**, 733-747.

Lawrence, G.W. and Cartwright, J.A. [2009] The initiation of sliding on the mid Norway margin in the Møre Basin. *Marine Geology*, **259(1-4)**, 21-35.

Løseth, H., Raulline, B. and Nygård, A. [2013] Late Cenozoic geological evolution of the northern North Sea: development of a Miocene unconformity reshaped by large-scale Pleistocene sand intrusion. *Journal of the Geological Society*, **170(1)**, 133-145.

Mazzini, A., Svensen, H. H., Planke, S., Forsberg, C. F. and Tjelta, T. I. [2016] Pockmarks and methanogenic carbonates above the giant Troll gas field in the Norwegian North Sea. *Marine Geology*, **373**, 26-38.

Millett, J. M., Manton, B. M., Zastrozhnov, D., Planke, S., Maharjan, D., Bellwald, B., ... and Birch-Hawkins, A. [2020] Basin structure and prospectivity of the NE Atlantic volcanic rifted margin: cross-border examples from the Faroe–Shetland, Møre and Southern Vøring basins. *Geological Society, London, Special Publications*, **495**.

Neagu, R. C., Cartwright, J., Davies, R. and Jensen, L. [2010] Fossilisation of a silica diagenesis reaction front on the mid-Norwegian margin. *Marine and Petroleum Geology*, **27(10)**, 2141-2155.

Nygård, A., Sejrup, H. P., Haflidason, H. and Bryn, P. [2005] The glacial North Sea Fan, southern Norwegian Margin: architecture and evolution from the upper continental slope to the deep-sea basin. *Marine and Petroleum Geology*, **22(1-2)**, 71-84.

Ottesen, D., Rise, L., Sletten Andersen, E., Bugge, T. and Eidvin, T. [2009] Geological evolution of the Norwegian continental shelf between 61° N and 68° N during the last 3 million years. *Norwegian Journal of Geology/Norsk Geologisk Forening*, **89(4)**.

Plaza-Faverola, A., Bünz, S. and Mienert, J. [2010] Fluid distributions inferred from P-wave velocity and reflection seismic amplitude anomalies beneath the Nyegga pockmark field of the mid-Norwegian margin. *Marine and Petroleum Geology*, **27(1)**, 46-60.

Polteau, S., Mazzini, A., Galland, O., Planke, S. and Malthe-Sørenssen, A. [2008] Saucer-shaped intrusions: Occurrences, emplacement and implications. *Earth and Planetary Science Letters*, **266(1-2)**, 195-204.

Riis, F., Berg, K., Cartwright, J., Eidvin, T. and Hansch, K. [2005] Formation of large, crater-like evacuation structures in ooze sediments in the Norwegian Sea. Possible implications for the development of the Storegga Slide. *Marine and Petroleum Geology*, **22**, 257-273.

Rise, L., Ottesen, D., Berg, K. and Lundin, E. [2005] Large-scale development of the mid-Norwegian margin during the last 3 million years. *Marine and Petroleum Geology*, **22(1-2)**, 33-44.

Schofield, N., Holford, S., Millett, J., Brown, D., Jolley, D., Passey, S.R., Muirhead, D., Grove, C., Magee, C., Murray, J. and Hole, M. [2017] Regional magma plumbing and emplacement mechanisms of the Faroe-Shetland Sill Complex: Implications for magma transport and petroleum systems within sedimentary basins. *Basin Research*, **29(1)**, 41-63.

Sejrup, H. P., Haflidason, H., Aarseth, I., King, E., Forsberg, C. F., Long, D. and Rokoengen, K. [1994] Late Weichselian glaciation history of the northern North Sea. *Boreas*, **23(1)**, 1-13.

Skjærpe, I., Tøllefsen, I. and Endresen, T. [2018] Developing Viper-Kobra: maximizing recovery by exploiting the unique characteristics of the sand injectite environment. In *80th EAGE Conference and Exhibition 2018*, **1**, 1-5.

Stoker, M.S., Holford, S.P. and Hillis, R.R. [2018]. A rift-to-drift record of vertical crustal motions in the Faroe–Shetland Basin, NW European margin: establishing constraints on NE Atlantic evolution. *Journal of the Geological Society*, **175(2)**, 263-274.

Tasianas, A., Bünz, S., Bellwald, B., Hammer, Ø., Planke, S., Lebedeva-Ivanova, N. and Krassakis, P. [2018] High-resolution 3D seismic study of pockmarks and shallow fluid flow systems at the Snøhvit hydrocarbon field in the SW Barents Sea. *Marine Geology*, **403**, 247-261.

Vétel, W. and Cartwright, J. [2010] Emplacement mechanics of sandstone intrusions: insights from the Panoche Giant Injection Complex, California. *Basin Research*, **22(5)**, 783-807.

Viana, A. R., Almeida, W., Nunes, M. C. V., & Bulhões, E. M. [2007] The economic importance of contourites. *Geological Society, London, Special Publications*, **276(1)**, 1-23.

www.npd.no, Norwegian Petroleum Directorate (NPD), Stavanger, Norway, 01.02.2022. Factpages of exploration wellbores, online. http://factpages.npd.no/factpages.

Figures and figure captions

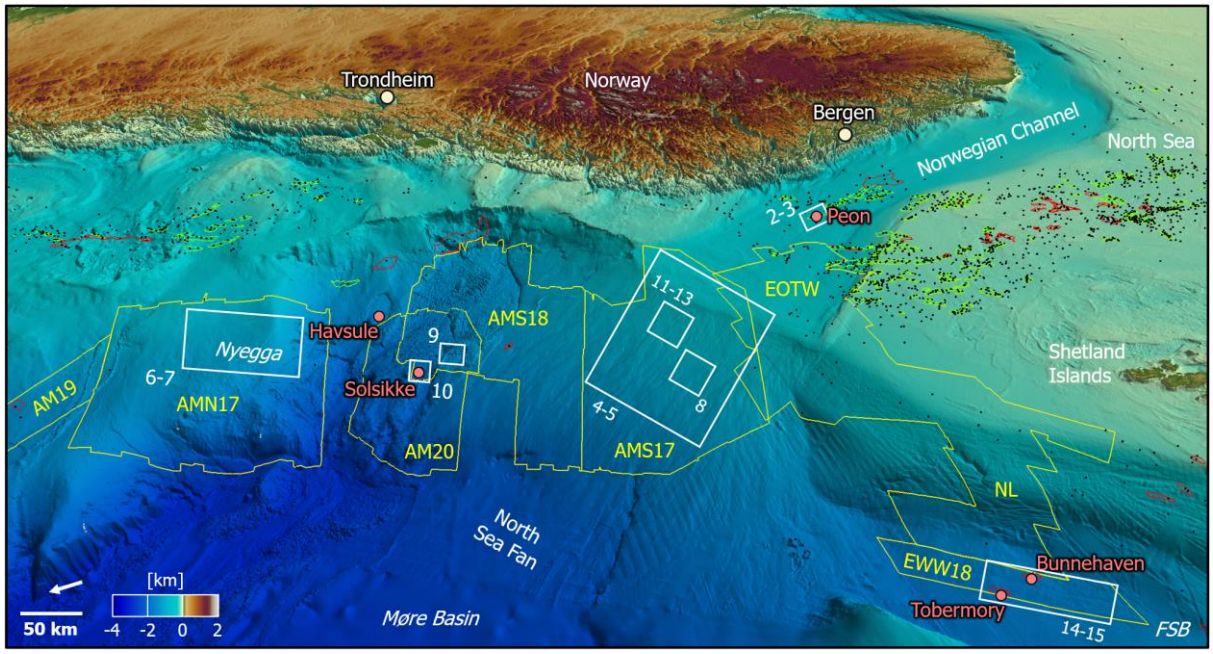

Fig. 1. *Location map of the Mid-Norwegian continental margin, North Sea Fan, northern North Sea, and Faroe-Shetland Basin (FSB) showing outline of interpreted 3D seismic cubes (yellow) and wells used in this study (red dots). Other wells (black dots), gas fields (red outlines), and oil fields (green outlines) are shown. White rectangles indicate the figure locations.*

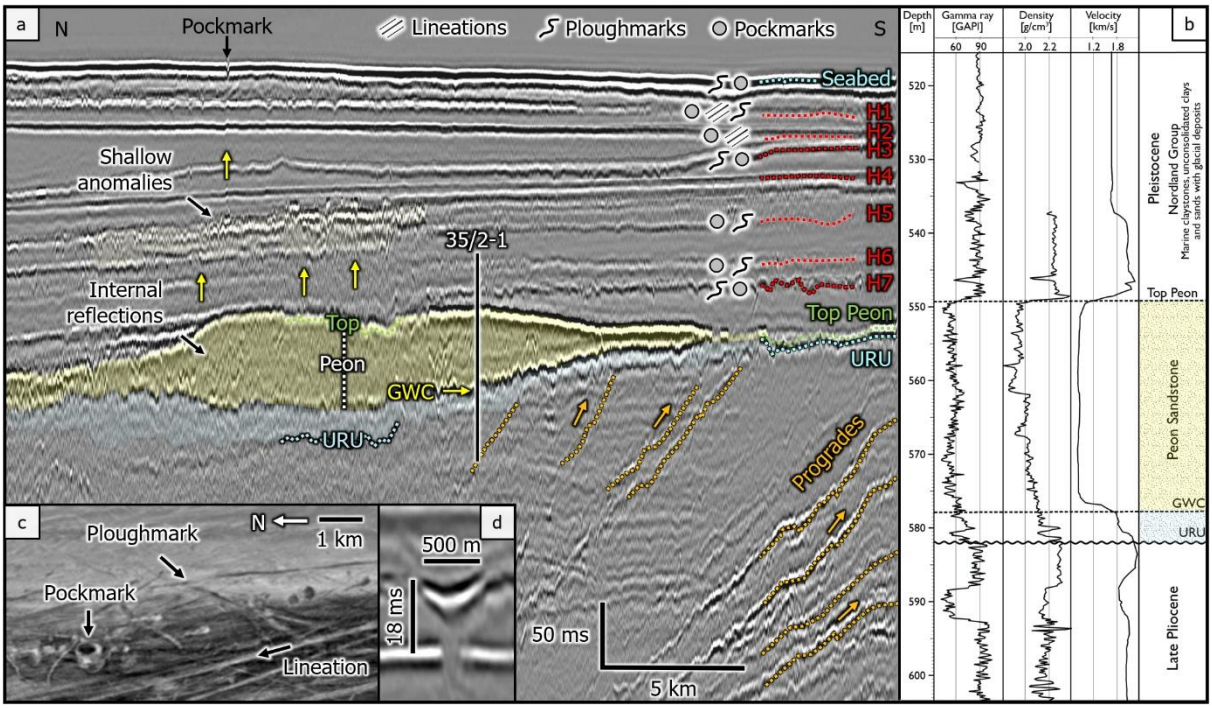

Fig. 2. *Glacial outwash fan forming the Peon gas discovery.* ***a)*** *High-resolution P-Cable profile showing the stratigraphic setting of Peon. H1-H7: Interpreted glacial horizons. Arrows indicate fluids charging the reservoir (orange) and fluid escape within the overburden (yellow). Black bar shows the location of the well log in Fig. 2b. Landform symbols are representative for the horizons.* ***b)*** *Well 35/2-1 through the Quaternary reservoir sandstone, which is characterized by a pronounced drop in density and velocity within the reservoir.* ***c)*** *Time slice across H1 showing buried landform assemblages.* ***d)*** *Seismic profile of pockmark shown in Fig. 2c. GWC: Gas-water contact annotated to the seismic profile at the well position, URU: Upper Regional Unconformity (glacial unconformity). Seismic data courtesy: Equinor.*

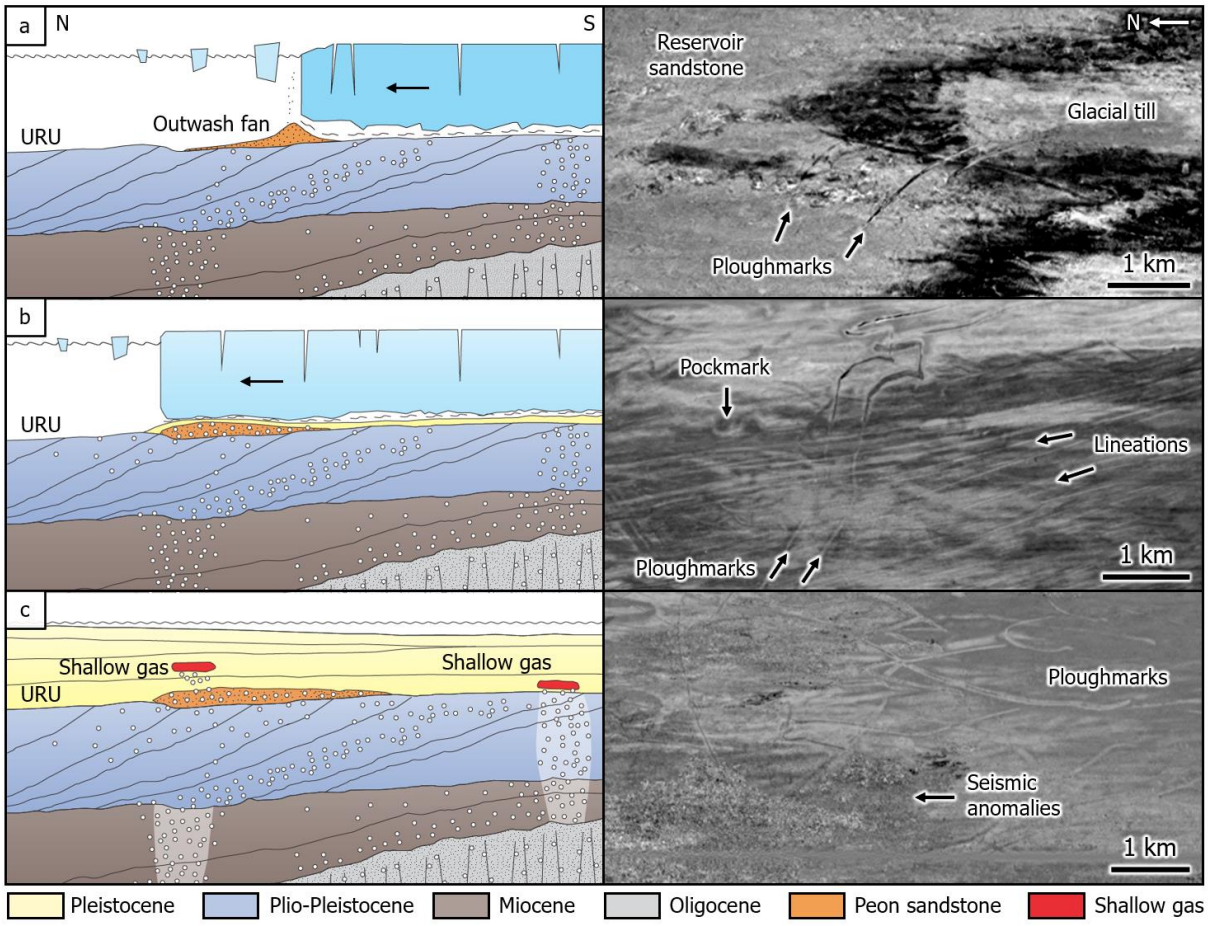

Fig. 3. *Sketch showing the formation of the Peon gas discovery (left) and seismic time slices (right).* ***a)*** *Deposition of the Peon sandstone. Time slice across central part of the reservoir.* ***b)*** *Sealing of the reservoir. Time slice across H3.* ***c)*** *Fluid migration above the reservoir. Time slice across H5. Fluid migration (white circles) and subglacial meltwater flow (black arrows) are indicated. URU: Upper Regional Unconformity (glacial unconformity). Seismic data courtesy: Equinor.*

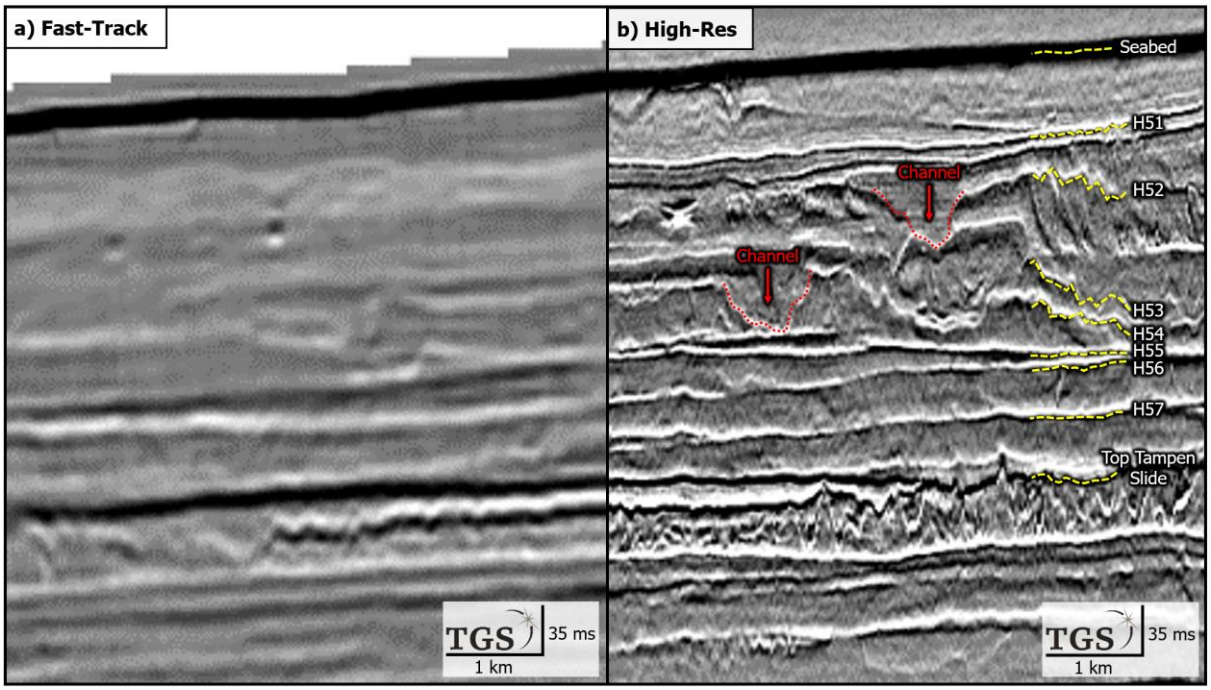

Fig. 4. *Comparison between* ***(a)*** *fast-track processed and* ***(b)*** *high-resolution processed 3D reflection seismic data of the uppermost stratigraphy of the North Sea Fan. Reflections H51-H57 indicate the seven surfaces characterized by channel-levee systems. Reflection H57 is gridded in Fig. 5. Examples of deep channels are shown by red stippled lines. Profile consists of fast-tracked processed data neighboring high-resolution processed data upslope.*

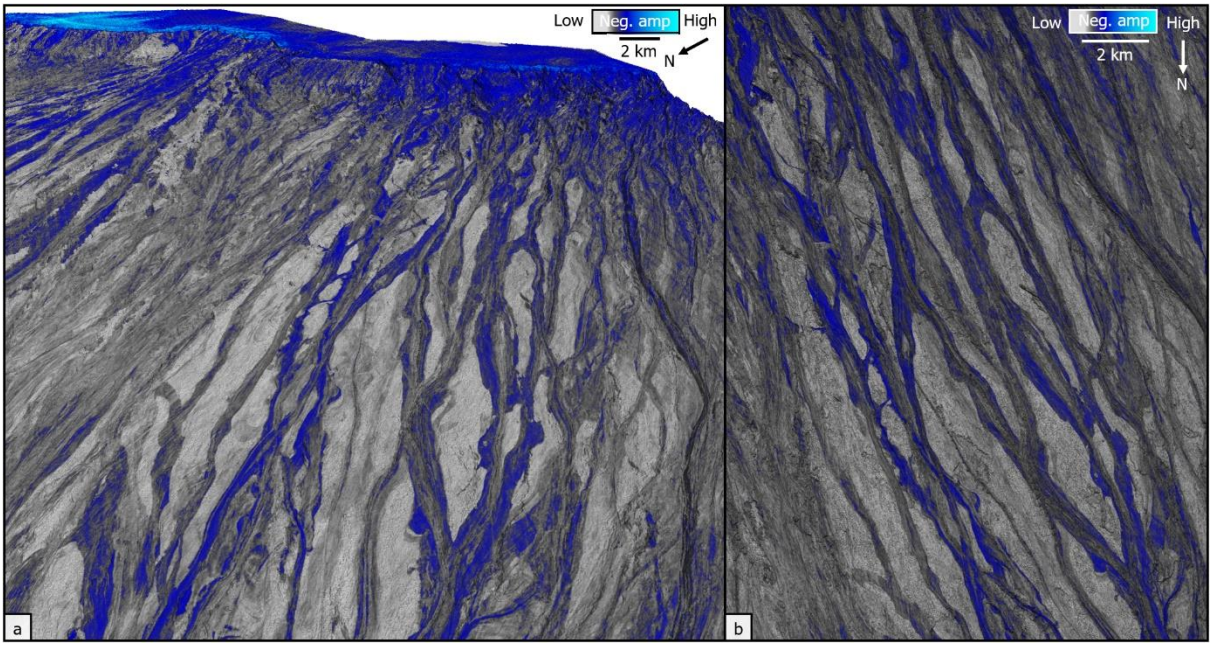

Fig. 5. *Meltwater turbidites of the North Sea Fan.* ***a)*** *3D view of H57 structure map draped by the minimum amplitude in a 20 ms window. The very high-amplitude bands (blue) are interpreted as channels of seismically distinct turbidite flows formed during shelf-edge glaciations.* ***b)*** *Seismic*

geomorphology of channel-levee systems. The levees have a lower impedance contrast (white) compared to the channels with a higher impedance contrast (blue). Seismic data courtesy: TGS.

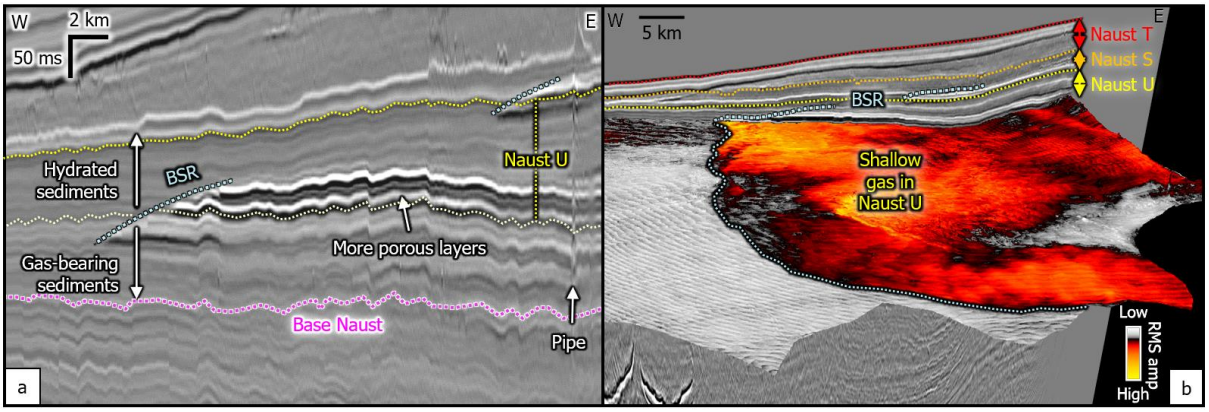

Fig. 6. *Gas-charged contourites within the Quaternary stratigraphy (here Naust Unit U) sealed by gas hydrates along the mid-Norwegian margin.* ***a)*** *Bottom simulating reflection (BSR) cross-cutting continuously deposited sediments, interpreted as glacimarine contourites. Strong seismic amplitudes represent stratigraphically-bound gas-charged layers.* ***B)*** *Naust Formation and its units are characterized by glacimarine sediments in AMN17. Surface shows RMS amplitude within Naust U. The BSR limits the western extent of the gas-charged layers. Seismic data courtesy: TGS.*

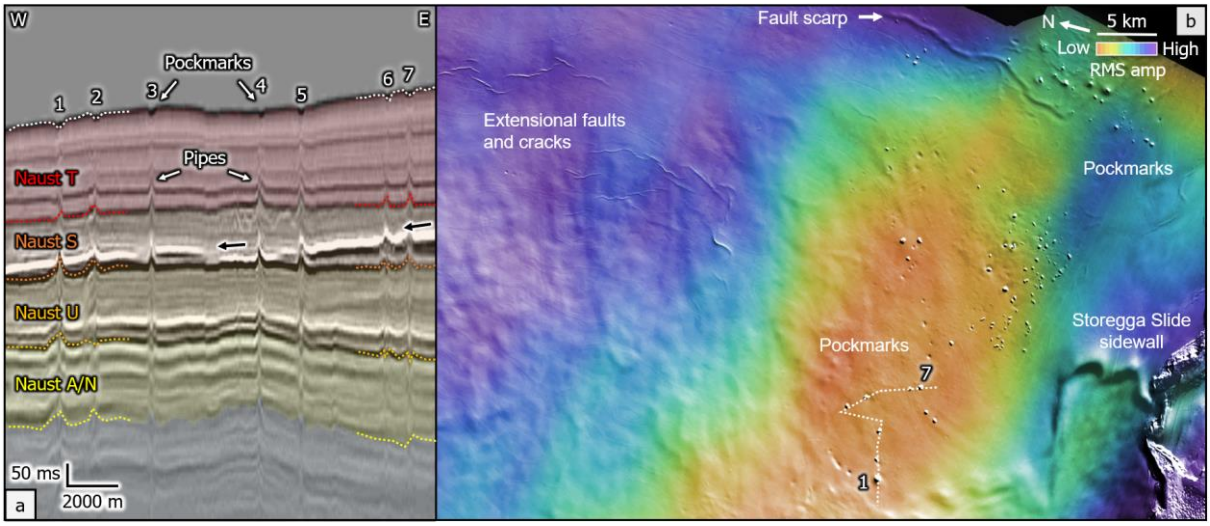

Fig. 7. *Association between indications of fluid escape features in the Quaternary and the seabed, and gas hydrates in the subsurface.* ***a)*** *Seismic profile showing the subunits of the Quaternary Naust Formation and pipe structures crossing a bottom simulating reflection (black arrow).* ***b)*** *Structure map of the seabed blended with RMS amplitude of the Naust S subunit. Pockmarks at the seabed correlate with low RMS amplitudes of Naust S subunit and pipes in the subsurface data. Seismic data courtesy: TGS.*

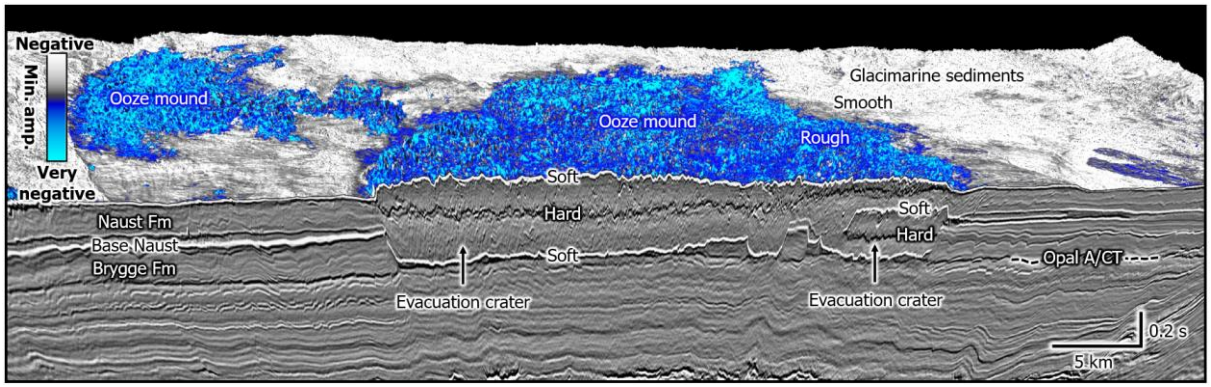

Fig. 8. *3D seismic chair view of remobilized oozes detected at the base of the Quaternary. Evacuation craters are expressed along the negative-amplitude Base Naust reflection. Note the very negative-amplitude reflection shaping rough remobilized ooze mounds above the craters and a positive-amplitude, chaotic reflection between the top ooze mound and the base of the evacuation craters. The horizon map is a blend of horizon structure and minimum amplitude. Seismic data courtesy: TGS.*

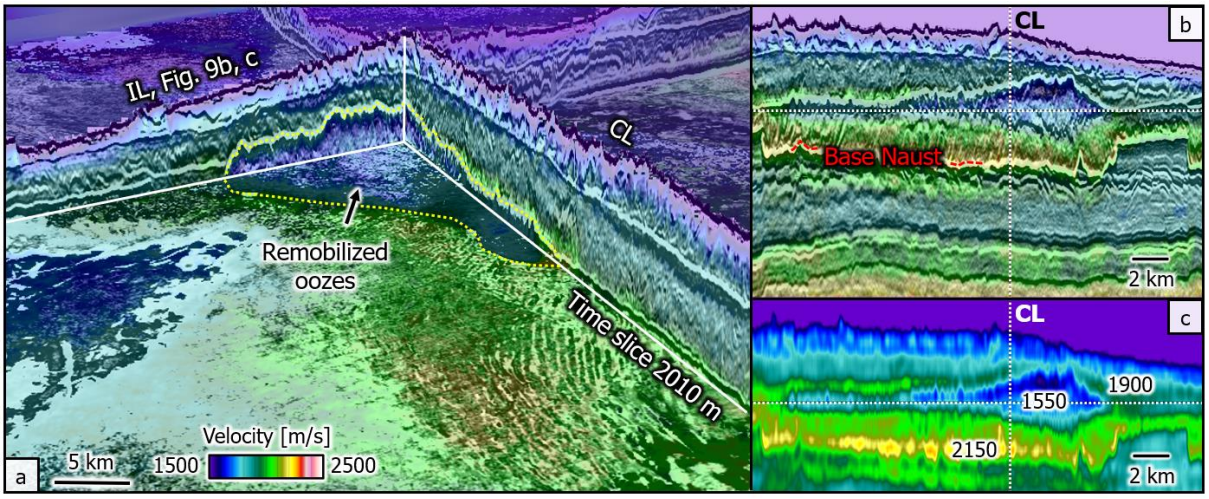

Fig. 9. *Lithological boundaries reflected in the Dynamic Matching Full Wave Inversion (DM FWI) velocity model, focusing on the stratigraphy around the remobilized oozes.* ***(a)*** *Chair view of inline (IL) and crossline (CL) of a remobilized ooze mound, characterized by a strong decrease in velocity compared to the surrounding glacigenic sediments.* ***(b)*** *Seismic profile and velocity model of ooze mound.* ***(c)*** *Velocity slow-down correlating with ooze mound. Seismic data courtesy: TGS.*

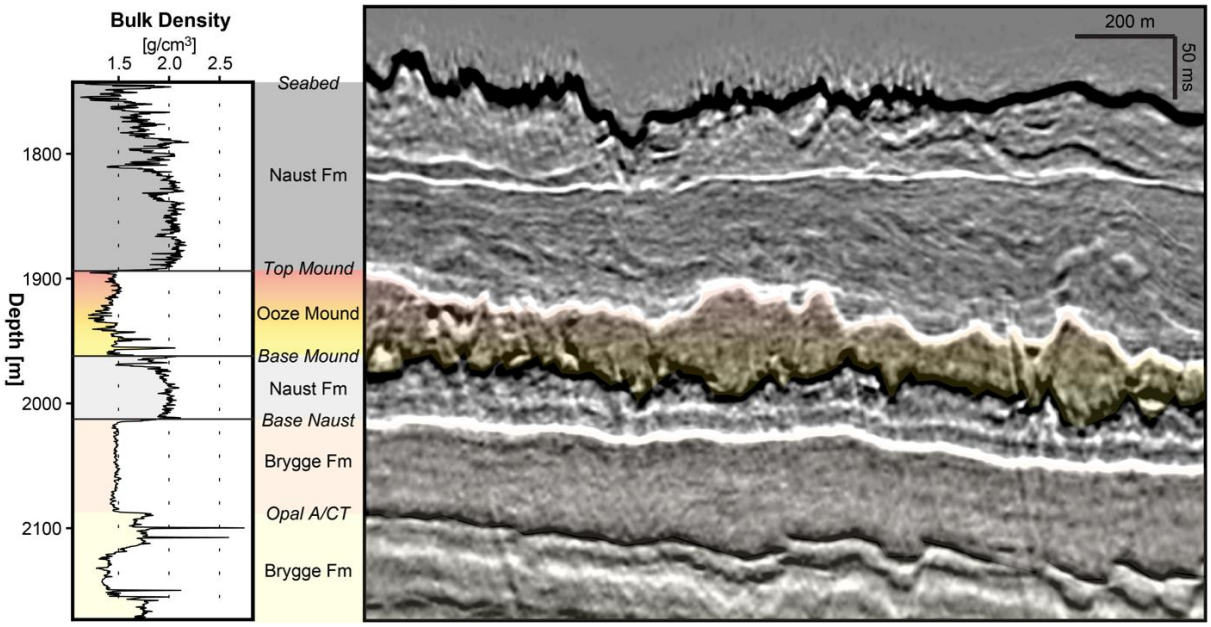

Fig. 10. *Tie of remobilized oozes into Solsikke well (6401/10-U1). Sedimentary units from the well are associated to the seismic units identified in a profile of the area. Ooze mound is characterized by low values in bulk density compared to the glacigenic sediments of the Naust Formation.*

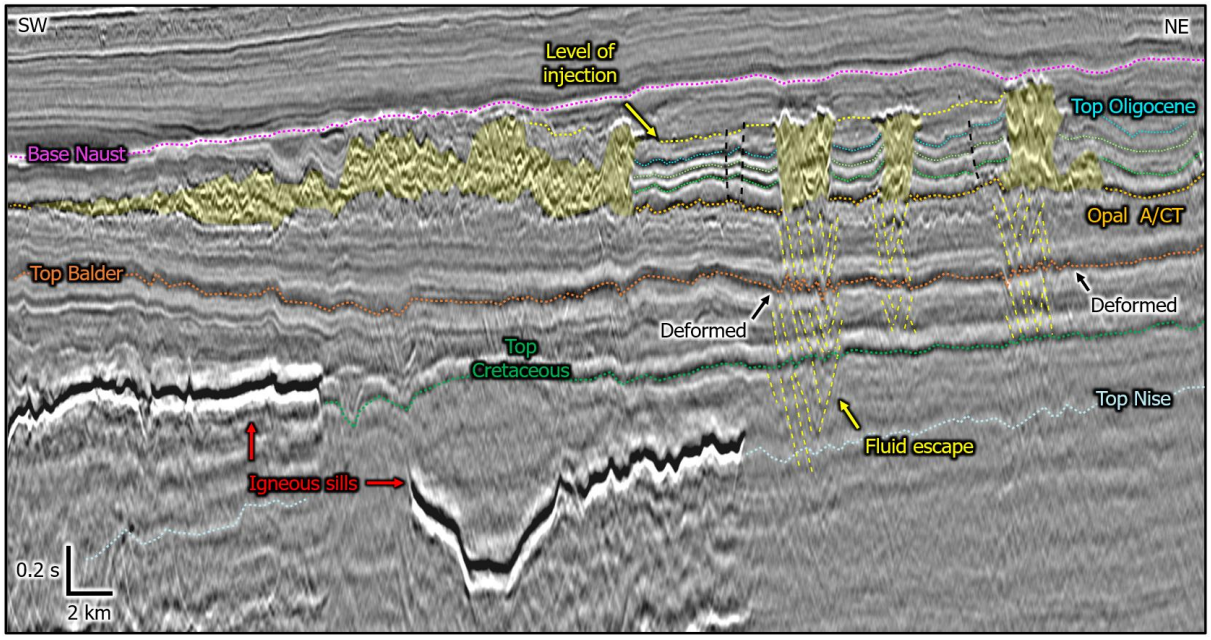

Fig. 11. *Sand injectites of the North Sea Fan. Seismic profile showing the upper Mesozoic and Cenozoic stratigraphy of the region, with sand injectites identified between the Opal A/CT reflection and the Base Naust reflection. Ages for key reflections are c. 2.6 Ma for Base Naust, early Eocene for Top Balder, and intra mid-Campanian for Top Nise. Seismic data courtesy: TGS.*

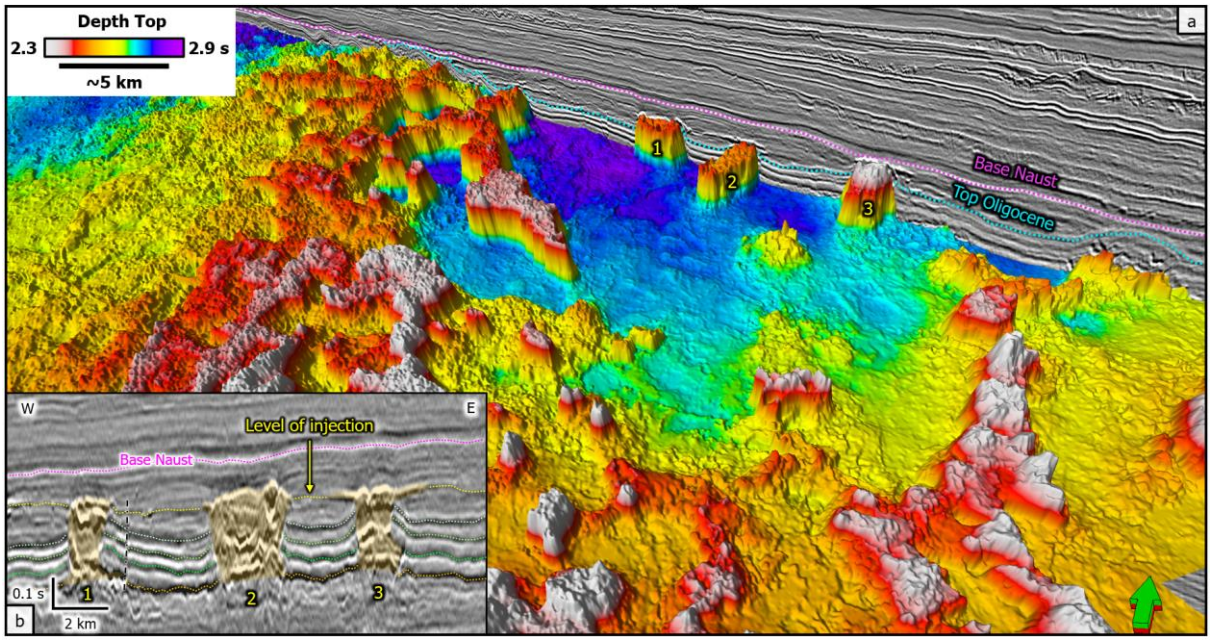

Fig. 12. *Seismic geomorphology of sand injectites in the North Sea Fan area.* ***a)*** *Chair view of the structure of the Top Injectites horizon with a seismic profile of the overlying stratigraphy.* ***b)*** *Seismic expression of three isolated injectite mounds with internal chaotic seismic facies (yellow). Seismic data courtesy: TGS.*

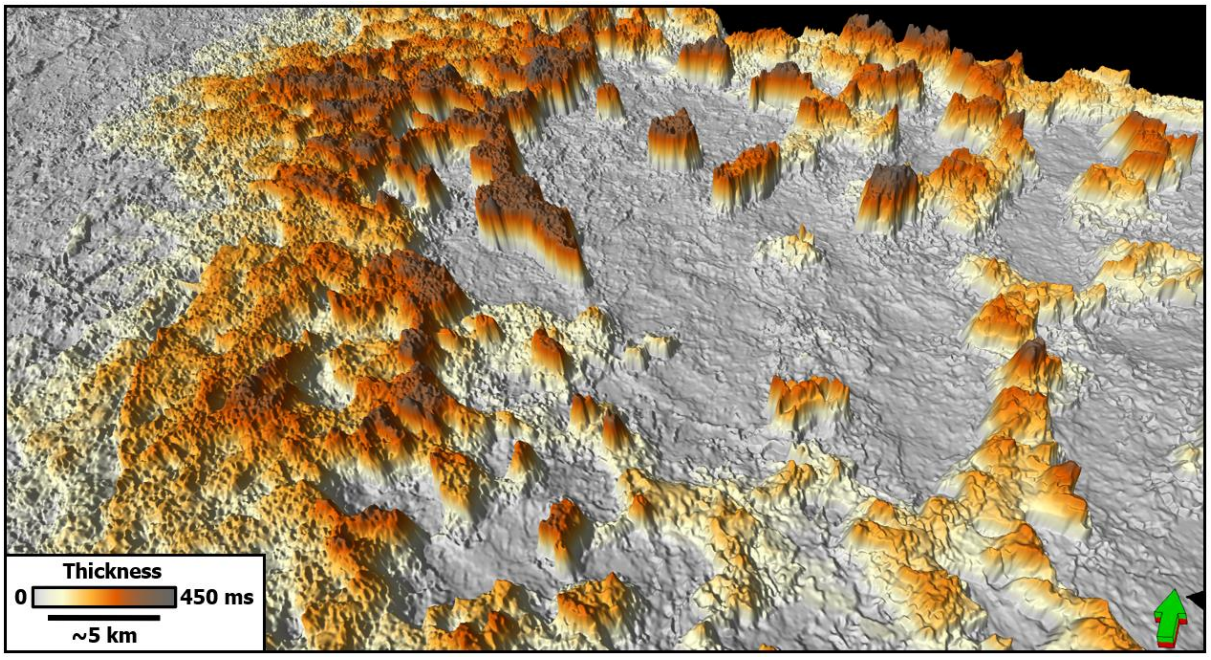

Fig. 13. *Thickness of sand injectites in the North Sea Fan area blended with the Top Injectite structure map. Seismic data courtesy: TGS.*

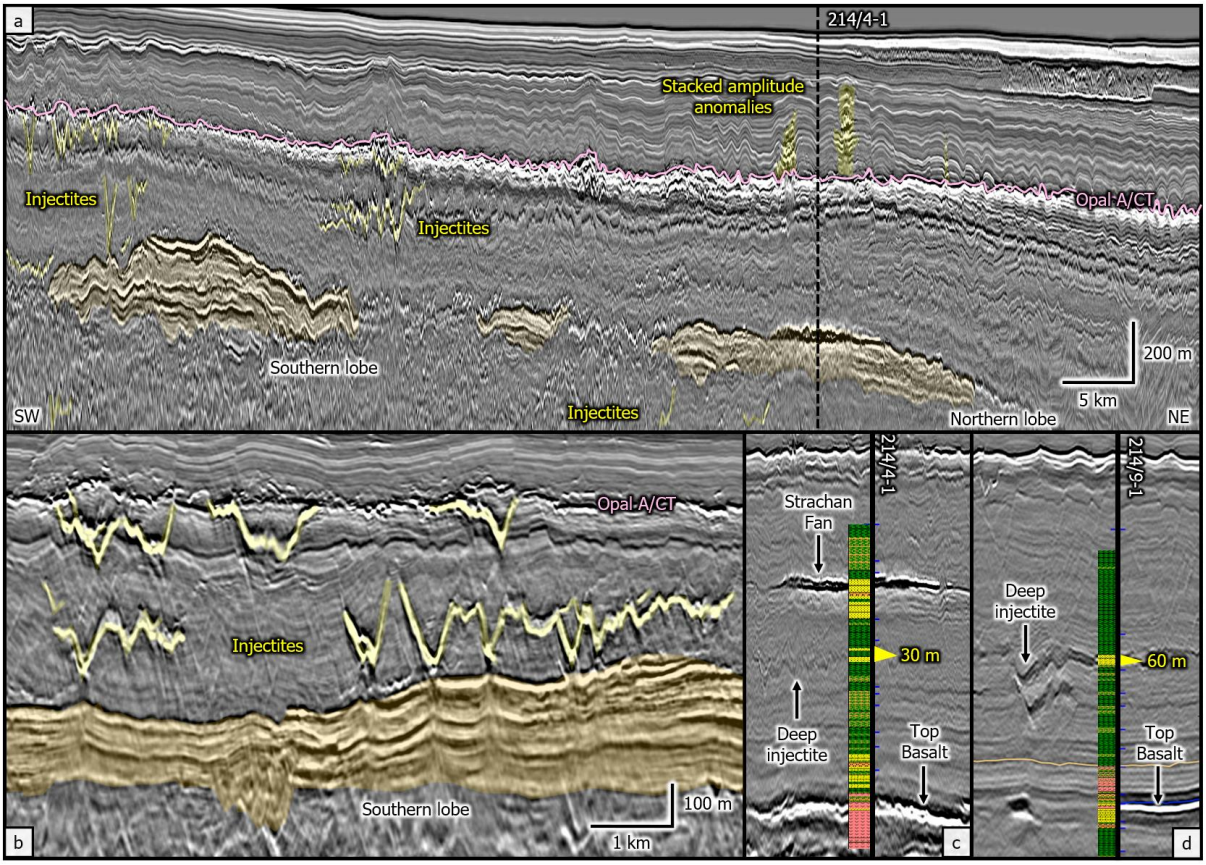

Fig. 14. *Sand injectites of the Strachan Fan area.* ***a)*** *Seismic profile across the lobes of the Strachan Fan (orange shapes) with injectites above the lobes (shallow injectites) and in the stratigraphy below (deep injectites).* ***b)*** *Relationship between the southern lobe (orange shape) and overlying sand injectites.* ***c)*** *Sandy lithology of the Strachan Fan and deeper injectites shown by the Tobermory well.* ***d)*** *Sandy lithology of injectite beds shown in the Bunnehaven well. Mudstone/shale (green), siltstone (orange), sandstone (yellow), and volcanic rocks (red) are shown in lithological logs from the TGS Facies Map Browser. Seismic data courtesy: TGS.*

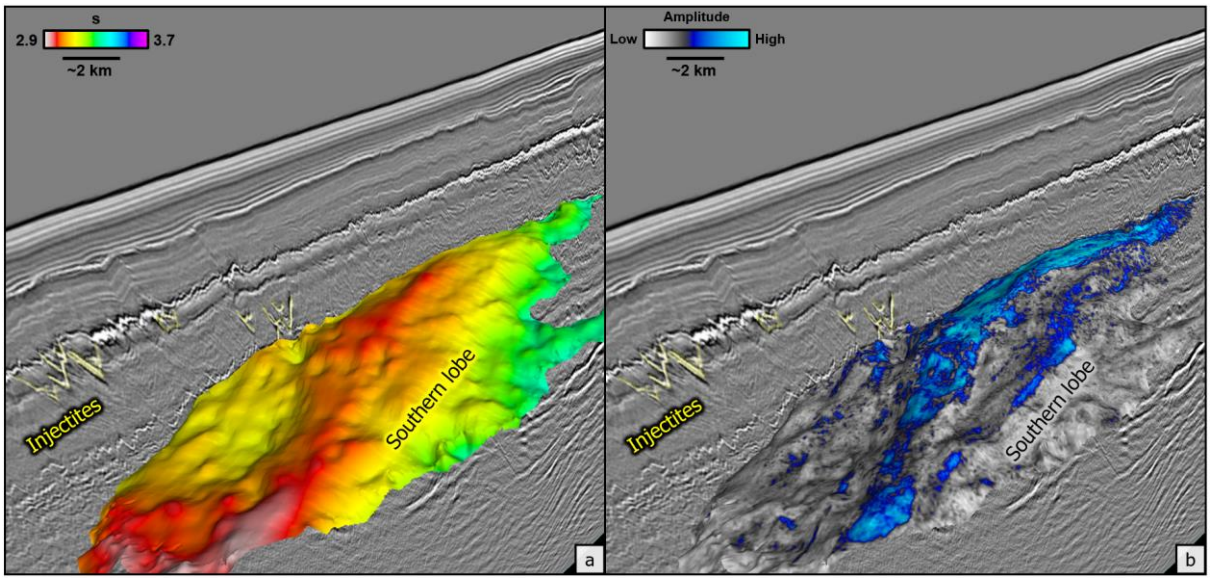

Fig. 15. *Implications of Strachan Fan on fluid flow.* ***a)*** *Structure of Top Strachan Fan with a seismic profile showing shallow injectites above (yellow).* ***b)*** *Blend of minimum amplitude with the Top Strachan Fan horizon with a seismic profile showing shallow injectites above (yellow). Seismic data courtesy: TGS.*

Tab. 1. *Quaternary and Neogene plays of the Norwegian Continental Shelf and the Faroe-Shetland Basin*

Play	**Age**	**Reservoir**	**Cap rock**	**Source rocks**
Glacial outwash fan	Quaternary	Glacial sands on paleo-shelf	Subglacial till and glacimarine sediments	Paleogene or older
Meltwater turbidites	Quaternary	Glacial sands in channel-levee systems on upper slope	Glacial muds, glacigenic debris flows and megaslides	
Gas hydrates	Quaternary	Glacial and glacimarine sediments	Trapped within hydrogen-bonded cages of water molecules	
Gas below gas-hydrate stability zone	Quaternary	Glacial and glacimarine sediments, commonly trapped by slide escarpments	Gas hydrates	
Contourites	Quaternary-Neogene	Sandy contourites	Muddy contourites and glacigenic debris flows	
Remobilized oozes	Neogene-Quaternary	Biosiliciclastic ooze mounds with associated evacuation craters	Muddy contourites, glacigenic debris flows and megaslides	
Sand injectites of Møre Basin	Neogene	Remobilized pre-Neogene sands	Marine mudstones	
Sand injectites of Faroe-Shetland Basin	Neogene	Remobilized pre-Neogene sands, associated to Strachan Fan	Marine mudstones	